Determining phonon deformation potentials of hexagonal GaN with stress modulation

Jun-Yong Lu,[1] Zhi-Jia Wang,[1] Dong-Mei Deng,[2] Yong Wang,[2] Kevin Jing Chen,[2] Kei-May Lau,[2] and Tong-Yi Zhang[1,a)]
[1]*Department of Mechanical Engineering, The Hong Kong University of Science and Technology, Clear Water Bay, Kowloon, Hong Kong, Special Administrative Region, China*
[2]*Department of Electronic and Computer Engineering, The Hong Kong University of Science and Technology, Clear Water Bay, Kowloon, Hong Kong, Special Administrative Region, China*

(Received 6 July 2010; accepted 2 November 2010; published online 28 December 2010)

In this work, phonon deformation potentials for E_2^H and $A_1(LO)$ phonons of epitaxial hexagonal GaN thin films grown by metalorganic chemical vapor deposition on Si (111) substrate were precisely determined with a stress modulation method, which was achieved via coin-shaped patterning of an originally flat film. By changing the size of patterned coin-shaped islands, the original biaxial stress in the flat film was reduced to different levels at the island centers, which was analyzed by finite element calculations. The proposed stress modulation method allows one to carry out a large number of Raman scattering tests, thereby leading to reliable results. With this method, the Raman biaxial pressure coefficients of E_2^H and $A_1(LO)$ phonons of GaN were determined to be 4.47 $\mathrm{cm}^{-1}/\mathrm{GPa}$ and 2.76 $\mathrm{cm}^{-1}/\mathrm{GPa}$, respectively. © *2010 American Institute of Physics*. [doi:10.1063/1.3524548]

I. INTRODUCTION

Gallium nitride (GaN) is one of the most promising semiconductor materials because of its tunable wide energy band when alloyed with AlN and InN, excellent electron transport property and outstanding inertness.[1] As one of its important applications, large scale production of GaN-based bright and energy-efficient white-light light-emitting diodes give revolutionary impacts to the illumination technology and may even crucially ameliorate our environment by decreasing the amount of fossil fuel used to produce electricity.[2]

However, residual stresses, which are detrimental to the performance of GaN-based devices,[3,4] usually exist in epitaxial GaN thin films due to lattice mismatch and/or thermal mismatch. To properly estimate residual stresses in synthesized GaN thin films with high spatial resolution, micro-Raman spectroscopy has been extensively implemented due to its simplicity and nondestructive nature, which requires precise values of phonon deformation potentials (PDPs) to link Raman shift or split to stress.[5] When a wurtzite crystal is biaxially deformed, hydrostatically deformed or uniaxially stressed along its c-axis, frequencies of E_2^H and $A_1(LO)$ phonons only shift.[5,6] The Raman shift is related to strain components ε_x, ε_y, and ε_z with PDP constants α and β, or $\tilde{\alpha}$ and $\tilde{\beta}$, by following expression:[5]

$$\Delta\omega^{\mathrm{GaN}} = 2\alpha\varepsilon_{xx}^{\mathrm{GaN}} + \beta\varepsilon_{zz}^{\mathrm{GaN}},$$

$$= 2\tilde{\alpha}\sigma_{xx}^{\mathrm{GaN}} + \tilde{\beta}\sigma_{zz}^{\mathrm{GaN}}. \quad (1)$$

where ε and σ denote strain and stress, respectively, and the z-axis is parallel to the crystalline c-axis. When $\sigma_{zz}^{\mathrm{GaN}}=0$, $\varepsilon_{xx}^{\mathrm{GaN}}=\varepsilon_{yy}^{\mathrm{GaN}}$, and $\sigma_{xx}^{\mathrm{GaN}}=\sigma_{yy}^{\mathrm{GaN}}$, the stress state is biaxial and Eq. (1) is reduced to:

$$\Delta\omega_b^{\mathrm{GaN}} = 2\tilde{\alpha}\sigma_{xx}^{\mathrm{GaN}} = \tilde{K}^B\sigma_{xx}^{\mathrm{GaN}}, \quad \textit{with}\ \tilde{K}^B = 2\tilde{\alpha}, \quad (2)$$

where the biaxial pressure coefficient $\tilde{K}^B$ is widely used to estimate the biaxial stress in GaN thin films, and thus is very important in practical applications.[7–9]

Besides some theoretical works,[6,10] limited experimental reports on the PDPs could be accessed in the literature.[6] As summarized in Table I, there is a considerable discrepancy among the reported PDPs of the E_2^H phonon mode of GaN.[13,15–17] This might be due to the difficulty in preparing GaN samples with different levels of biaxial stress so that only limited numbers of experimental data in Raman shift versus stress were available. The Raman shift in the $A_1(LO)$ mode in GaN crystals is particularly important in resonant scattering and thus the Raman biaxial pressure coefficient is very critical.[14] However, only two values of PDP of the $A_1(LO)$ mode have been reported with a great discrepancy (0.9 and 1.91 $\mathrm{cm}^{-1}/\mathrm{GPa}$). Clearly, large number of tests should be conducted to have reliable values of PDPs of GaN crystals.

In the present work, stress modulation via coin-shaped patterning method was proposed, with which biaxially stress state at different relaxed levels could be assigned by finite element analysis (FEA) and realized by using the microfabrication technique. Thus, it becomes possible to experimentally determine Raman biaxial pressure coefficients of E_2^H and $A_1(LO)$ phonon modes of GaN crystals, thereby leading to reliable PDPs.

II. EXPERIMENTS

In this study, nominally undopped GaN epitaxial layers were grown by metal-organic chemical vapor deposition (MOCVD) on Si (111) substrates in an Aixtron 2000HT system. Trimethylgallium, trimethylaluminum, and ammonia (NH_3) were used as precursors for Ga, Al, and N, respec-

a)Electronic mail: mezhangt@ust.hk.

0021-8979/2010/108(12)/123520/5/$30.00

TABLE I. Summary of reported $\widetilde{K}$ values for the E_2^H and $A_1(LO)$ phonon modes of hexagonal GaN crystals.

Calibration method	Growth technology	Heterostructure	Elastic constants used (GPa if any)	$\widetilde{K}^B$ (cm^{-1}/GPa) E_2^H	$\widetilde{K}^B$ (cm^{-1}/GPa) $A_1(LO)$
Ab initio calculations	⋯	⋯	⋯	~2.4 [a,b]	⋯
Biaxial bending	MOCVD	GaN/Si	Several sets of elastic constants	1.7 ± 0.1 [c]	⋯
Curvature	MOVPE	GaN/AlN/sapphire	$E=196$, $\gamma=0.3$	6.2[d]	⋯
Reflection for excitonic transition	MOVPE	GaN/sapphire	$C_{11}=296$, $C_{12}=130$, $C_{13}=158$, $C_{33}=267$	2.9[e]	0.9[e]
XRD	MBE	GaN/(HT)AlN/GaN/AlN/Si	$C_{11}=390$, $C_{12}=145$, $C_{13}=106$, $C_{33}=398$	2.43[f]	1.91[f]
	MOCVD	GaN/6H–SiC	$C_{11}=390$, $C_{12}=145$, $C_{13}=106$, $C_{33}=398$	2.7[g]	⋯
	MBE	GaN/(LT)GaN/sapphire	$E=290$, $B=200$, $\gamma=0.23$	4.2 ± 0.3 [h]	⋯
	MOCVD	GaN/AlN/sapphire			
	MOCVD	GaN/(LT)GaN/sapphire			
This work	MOCVD	GaN/AlN/Si	$E=287$, $\gamma=0.347$	4.47	2.76

[a]Reference 6.
[b]Reference 7.
[c]Reference 11.
[d]Reference 12.
[e]Reference 13.
[f]Reference 14.
[g]Reference 15.
[h]Reference 16.

tively, and H_2 was used as carrier gas. Prior to the deposition, Si substrates were heated up to 1180 °C for 10 min under H_2 ambient to remove the native oxide on the Si surfaces. Then, an AlN nucleation layer (~40 nm) was deposited, followed by the growth of 1-μm-thick GaN layer. Biaxial residual stress in the GaN epitaxial layer was determined to be 1167.29 ± 146.37 MPa with an optical stress meter (Scientific Measurement Systems, Inc., Model SMSi 3800).

As shown in Fig. 1, with the synthesized GaN samples, coin-shaped islands with radius ranging from 3 to 60 μm were fabricated by using inductively coupled plasma reactive ion etching with SiO_2 as hardmask, whereas the 0.3 μm SiO_2 layer was deposited onto the samples with plasma enhanced chemical vapor deposition system (Allwin 21 Corp., STS 310PC PECVD). The spacing between the islands was larger than at least twice of the island diameter, which was sufficient to eliminate interference between them.

With Renishaw Invia RM3000 Raman spectrometer and 50× objectives, Raman measurements were performed at ambient temperature in backscattering geometry using a 514 nm air-cooled Ar^+ laser as an excitation source. With 65 μm slit-width of the spectrometer, the accuracy of the Raman measurement is 0.2 cm^{-1}. Meanwhile, the excitation power was 1.25 mW on the sample surface, corresponding to an excitation power density of around 1.6×10^5 W/cm^2 to avoid any potential local heating. Moreover, as shown in Fig. 2, the incident beam was focused at the island center where biaxial stress exists. Raman spectrum was measured four times for average at every island center. Moreover, the $z(x,x)\bar{z}+z(x,y)\bar{z}$ back scattering geometry mainly selects the

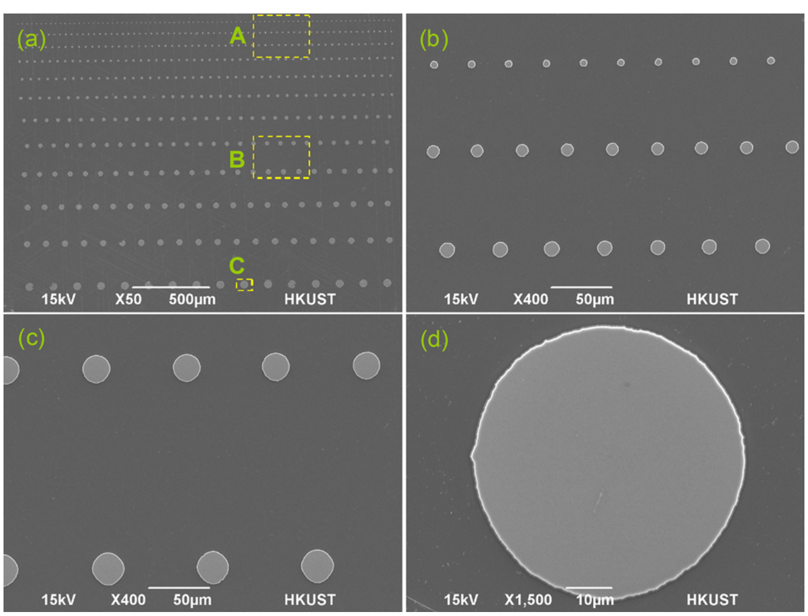

FIG. 1. (Color online) (a) Fabricated array of coin-shaped GaN islands. Close-up views at regions A, B, and C in (a) are given in (b), (c), and (d), respectively. The island radiuses are approximately 3, 5, and 6 μm in (a), 11 and 13 μm in (b), and 31 μm in (c).

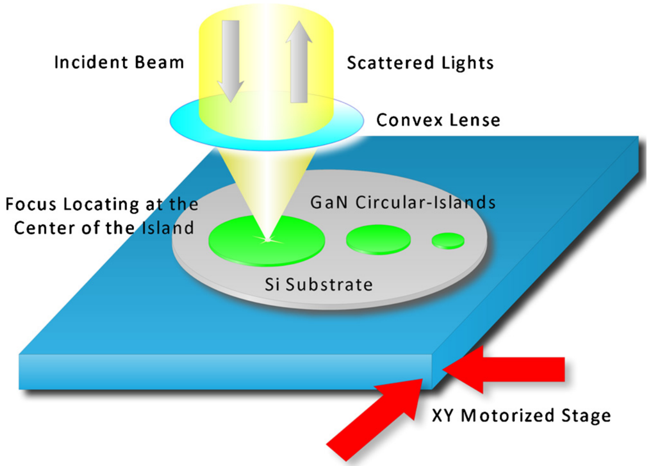

FIG. 2. (Color online) Schematic illustration of the experimental setup.

E_2^H and $A_1(LO)$ phonon modes. Lorentzian fitting was used to determine the precise peak positions from raw data.

III. ANALYSIS

In the present study, stress analysis was carried out on one single GaN island, with its bottom bonded to the Si substrate and its lateral sides traction-free. FEA was conducted with commercial software ANSYS V10.0 and 20-node quadratic solid186 element. For simplicity, both of GaN thin film and Si substrate were assumed to be mechanically isotropic. Young's modulus of 185 GPa and Poisson's ratio of 0.26 were used for the Si (111) substrate.[18] The Young's modulus of 287 GPa of the as-prepared GaN thin films determined from the microbridge test[17] and Poisson's ratio of 0.347 (Ref. 19) were used in the FEA. Since linear elasticity was used in the FEA, the original biaxial stress in the flat film was set to be 1 GPa to simplify the final normalization process. The number of elements ranged from 45 758 to 119 305 as the island size increased from 3 to 60 μm. Due to geometric symmetry, biaxial stress maintains at the coin-shaped island centers.

The FEA shows that when the spacing between adjacent islands is larger than twice the island diameter, the interaction between them could be ignored (<0.5%), which is the guideline in the design of coin-shaped patterns.

As an example, Fig. 3 shows FEA results for an island of radius R=25 μm. Figure 3(a) illustrates the in-plane stress along radial orientation (σ_r), and the close-up view of σ_r-distribution is given in Figs. 3(b) and 3(c). The σ_r stress component is tensile almost everywhere in the island except the edge part where stress concentration occurs. Figure 3(d) shows the in-plane normal stress components σ_r and σ_θ, at the bottom and surface of the island, as a function of distance from the center. At and near the island center, as expected, $\sigma_r = \sigma_\theta$ and the stress at the surface is the same as that on the bottom face, illustrating the biaxial stress state. However, stresses at the island edge vary greatly.

Figure 4 shows the biaxial stress at the island center versus the island radius, indicating an exponential decay of the original stress in the flat film. When the island radius is 3 μm, the biaxial stress at the center is only 32% of the

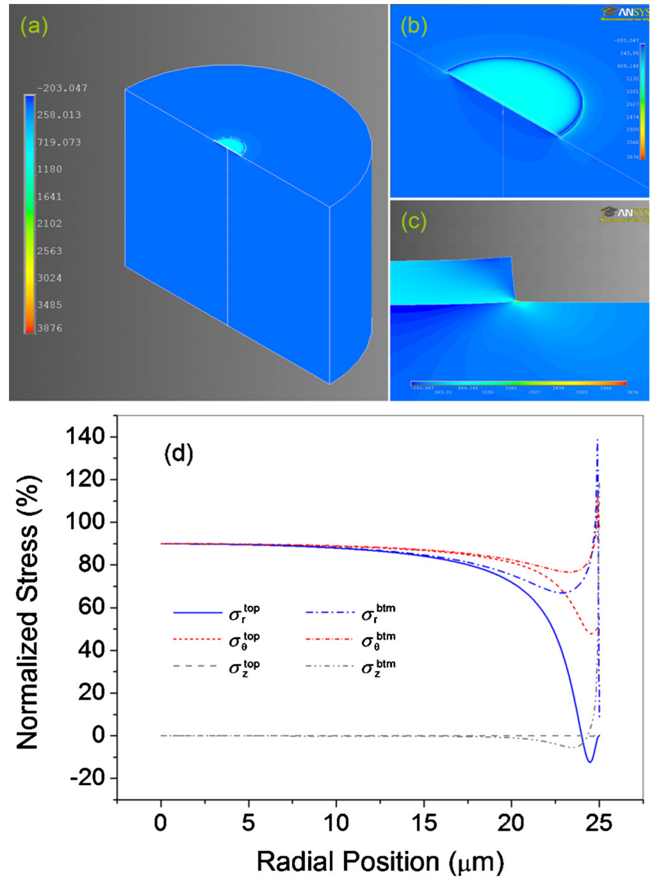

FIG. 3. (Color online) (a) Spatial distribution of σ_r in the GaN/Si bilayer system (R=25 μm). (b) Close-up views of the stress field (σ_r). (c) Stress concentration at the edge of the island. (d) Stress distribution along the radial direction at top surface and bottom interface of the coin-shaped GaN island.

original level, meaning 68% of the original stress is released. The original biaxial stress is also relaxed in the thickness direction. The inset in Fig. 4 shows the normalized biaxial stress evolves from the bottom interface to the top free surface at the center point. Circles in Fig. 4 indicate the average values of the biaxial stress over the thickness direction of the thin film. The biaxial stress may vary greatly along the thick-

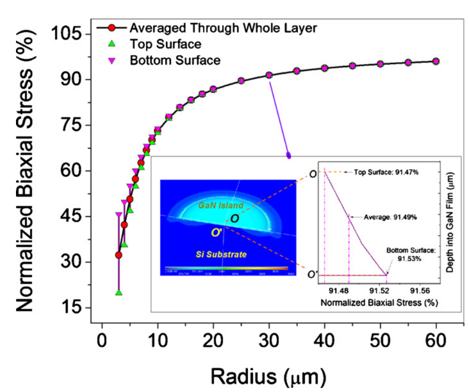

FIG. 4. (Color online) Normalized biaxial stress, from FEA, at the island center vs the island radius, where the triangles indicate the normalized stress level at top surface and bottom interface at the island center and the circles show the average stress level on the point all through the vertical axis. The inset shows one example (R=30 μm) of depth dependence of relaxed stress.

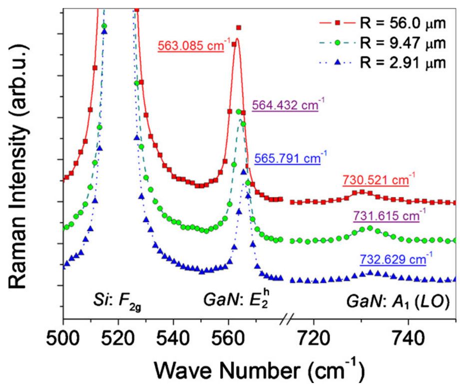

FIG. 5. (Color online) Raman spectra captured at centers of the coin-shaped islands with distinct radiuses.

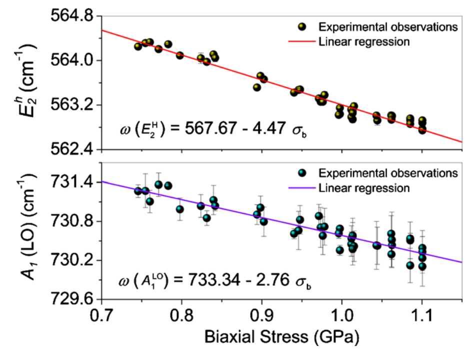

FIG. 6. (Color online) Linear relationship between observed E_2^H and $A_1(LO)$ phonon frequencies and biaxial stress.

ness direction in the coin-shaped islands with radius smaller than 7 μm. Therefore, only the FEA results and Raman data for coin-shaped islands with radiuses larger than 7 μm were chosen for further analysis to enhance the analysis reliability.

Based on linear elasticity, biaxial stress at each of the island centers was calculated by multiplying the normalized stress, shown in Fig. 4, with the original film stress, which was measured in the present work by using the curvature method.

IV. RESULTS AND DISCUSSION

Wurtzite GaN crystal belongs to the C_{6v}^4 space-group and its first-order zone-center ($\Gamma=0$) phonon normal modes can be specified into eight sets, i.e., $2A+2E_1+2E_2+2B_1$ modes. Besides acoustic sets A_1+E_1, the remaining ones are optical vibrations, among which the $2B_1$ modes are silent.[5] In our experiments, backscattering geometry was adopted and the incident light propagated along the [0001] direction, therefore E_2 and $A_1(LO)$ modes were allowed from the selection rules.[20]

As an example, Fig. 5 shows the Raman spectra taken at centers of the coin-shaped islands of radiuses 56, 9.47, and 2.91 μm. The Raman spectra from the 2.91 μm-diameter inland shown in Fig. 5 is not used in the flowing analysis because the variation of biaxial stress in the thickness direction, as mentioned above. Besides the strong peaks of F_{2g} mode of silicon (about 520 cm^{-1}), the E_2^H (about 564 cm^{-1}) and the $A_1(LO)$ (about 732 cm^{-1}) phonons of GaN could be clearly identified. Both of E_2^H and $A_1(LO)$ phonon frequencies increased as the island radius became larger. This is because the biaxial stress level at the center of a larger island is higher than that in smaller island, as shown by Fig. 4 and reported in Refs. 21 and 22. In addition, Fig. 5 also shows that the full width at half maximum of the E_2^H and $A_1(LO)$ phonon lines are typically 3.83 cm^{-1} and 5.45 cm^{-1}, respectively, insensitive to the island size.

Figure 6 demonstrates E_2^H and $A_1(LO)$ phonon frequencies as functions of the biaxial stress, indicating clearly linear relationship for both phonon modes. The error bar of E_2^H phonon is smaller than that of $A_1(LO)$. This is because the former phonon has a much larger scattering cross section. Linear fitting the experimental data gives:

$$\omega_{E_2^H} = 567.67 - 4.47\sigma_b, \tag{3a}$$

$$\omega_{A_1(LO)} = 733.34 - 2.76\sigma_b. \tag{3b}$$

For E_2^H mode vibration, the Raman biaxial pressure coefficient is measured to be 4.47 cm^{-1}/GPa, which is quite close to one of the most widely used values, 4.2 ± 0.3 cm^{-1}/GPa.[16] As mentioned above, the stress modulation method allows us to conduct the Raman tests over 40 different values of stresses so that the experimental results are more reliable. For the $A_1(LO)$ phonon mode, the Raman biaxial stress coefficient was only experimentally calibrated twice with the values of 0.9 (Ref. 13) and 1.91 cm^{-1}/GPa.[14] The present value of 2.76 cm^{-1}/GPa is closer to the latter value.

Furthermore, as stated in Eq. (1), Raman shift in GaN crystals may be expressed in terms of strain components ε_x, ε_y, and ε_z and PDPs α and β:

$$\Delta\omega = \alpha(\varepsilon_x+\varepsilon_y)+\beta\varepsilon_z. \tag{4}$$

To determine the values of α and β, we use the Raman biaxial pressure coefficients determined in the present work and the Raman hydrostatic pressure coefficients, which was experimentally reported by Perlin *et al.*[23] ($\tilde{K}^H_{E_2^h}$ $=4.17$ cm^{-1}/GPa) and Goñi *et al.*[24] ($\tilde{K}^H_{E_2^h}=4.24$ cm^{-1}/GPa and $\tilde{K}^H_{A_1(LO)}=4.40$ cm^{-1}/GPa). Thus, two equations could be written for solving the PDPs,[13] i.e.,

$$2(S_{11}+S_{12})\alpha + 2S_{13}\beta = -\tilde{K}^B, \tag{5a}$$

$$2(S_{11}+S_{12}+S_{13})\alpha + (2S_{13}+S_{33})\beta = -\tilde{K}^H, \tag{5b}$$

where S_{ij} are compliances of GaN crystals and S_{ij} are related to elastic constants C_{ij} by:

$$S_{11} = \frac{-C_{13}^2 + C_{11}C_{33}}{(C_{11}-C_{12})[-2C_{13}^2+(C_{11}+C_{12})C_{33}]}, \tag{6a}$$

$$S_{12} = \frac{C_{13}^2 - C_{12}C_{33}}{(C_{11}-C_{12})[-2C_{13}^2+(C_{11}+C_{12})C_{33}]}, \tag{6b}$$

$$S_{13} = \frac{C_{13}}{2C_{13}^2-(C_{11}+C_{12})C_{33}}, \tag{6c}$$

TABLE II. Calculated PDPs of E_2^H and $A_1(LO)$ phonon of hexagonal GaN at room temperature. (α and β are in unit of cm^{-1}.)

Phonon symmetry	α (cm^{-1})	β (cm^{-1})
E_2^H	-1063.95[a]	-352.08[a]
	-1071.23[b]	-378.4[b]
$A_1(LO)$	-846.76[b]	-903.68[b]

[a]With Raman hydrostatic pressure coefficient reported by Perlin *et al.*, Ref. 23.
[b]With Raman hydrostatic pressure coefficient reported by Goñi *et al.*, Ref. 24.

$$S_{33} = \frac{C_{11} + C_{12}}{-2C_{13}^2 + (C_{11} + C_{12})C_{33}}. \tag{6d}$$

With the elastic constants given in Ref. 19 ($C_{11}=390$ GPa, $C_{12}=145$ GPa, $C_{13}=106$ GPa, $C_{33}=398$ GPa), we calculated the values of α and β for the two phonon modes and also tabulated them in Table II. Then, Eq. (4) with the calculated results of α and β (particularly the $A_1(LO)$ mode) allows one to estimate the Raman shift at a more general strain state.

Additionally, it is interesting to notice that the present extrapolated E_2^H frequency for stress-free GaN is 567.67 cm^{-1}, just between with experimentally reported E_2^H frequencies of 568 (Ref. 23) and 567.6 cm^{-1}.[25] For the stress-free $A_1(LO)$ phonon frequency, the reported experimental value is the same as the theoretical prediction to be 734.0 cm^{-1}.[25] The present extrapolated value of 733.34 cm^{-1} is very close to the reported value.[25] Although the modulated biaxial stress range (minimum biaxial stress $\sigma_{Min}^b=746$ MPa) is far away from the stress-free state, the fact that extrapolated intercepts from above expressions are satisfactorily consistent with the reported values calculated and/or measured from bulk samples indicates the validation of the proposed approach.

V. SUMMARY

(1) Stress modulation method was proposed via patterning coin-shaped islands. By combining microfabrication techniques and three-dimensional numerical simulation, effective stress modulation is achieved with both of large modulation range (up to 35% of the original residual stress) and elaborate stress increments (about 15 MPa in this study). This method is powerful in experimentally calibrating PDPs of materials and in studying strain-induced phenomena of thin films.

(2) With this stress modulation method, we studied the stress induced first-order Raman phonon frequencies of hexagonal GaN. The biaxial stress dependences of Raman frequencies were determined to be $(567.67-4.47\sigma_b)$ cm^{-1} and $(733.34-2.76\sigma_b)$ cm^{-1} for E_2^H and $A_1(LO)$ modes, respectively. The extrapolated intercepts of the stress-free phonon frequencies (567.67 cm^{-1} for E_2^H phonon and 733.34 cm^{-1} for $A_1(LO)$ phonon) are very close to the reported values. Furthermore, general PDPs of α and β were calculated by combining these observed Raman biaxial pressure coefficients with the Raman hydrostatic pressure coefficients.

ACKNOWLEDGMENTS

This research was financially supported by RGC Central Allocation Research Grant, Grant No. CA-07/08.EG02. One of the authors (Jun-Yong LU) would like to thank Professor Manuel Cardona, Dr. Razvigor Ossikovski, and Professor Linda S. Schadler for inspirable discussions, and Dr. Bo-Rong SHI and Mr. Zhao-Jun LIU for fruitful technical help.

[1]S. N. Mohammad, A. Salvador, and H. Morkoc, Proc. IEEE **83**, 1306 (1995).
[2]P. Y. Yu and M. Cardona, *Fundamentals of Semiconductors: Physics and Materials Properties* (Springer-Verlag, Berlin, 2003).
[3]L. Liu and J. H. Edgar, Mater. Sci. Eng. R. **37**, 61 (2002).
[4]S. Nakamura, Semicond. Sci. Technol. **14**, R27 (1999).
[5]R. J. Briggs and A. K. Ramdas, Phys. Rev. B **13**, 5518 (1976).
[6]J.-M. Wagner and F. Bechstedt, Appl. Phys. Lett. **77**, 346 (2000).
[7]V. V. Chaldyshev, F. H. Pollak, M. Pophristic, S. P. Guo, and I. Ferguson, J. Appl. Phys. **92**, 6601 (2002).
[8]F. Furtmayr, M. Vielemeyer, M. Stutzmann, A. Laufer, B. K. Meyer, and M. Eickhoff, J. Appl. Phys. **104**, 074309 (2008).
[9]D. M. Deng, N. S. Yu, Y. Wang, X. B. Zou, H. C. Kuo, P. Chen, and K. M. Lau, Appl. Phys. Lett. **96**, 201106 (2010).
[10]J.-M. Wagner and F. Bechstedt, Phys. Rev. B **66**, 115202 (2002).
[11]A. Sarua, M. Kuball, and J. E. Van Nostrand, Appl. Phys. Lett. **85**, 2217 (2004).
[12]T. Kozawa, T. Kachi, H. Kano, H. Nagase, N. Koide, and K. Manabe, J. Appl. Phys. **77**, 4389 (1995).
[13]F. Demangeot, J. Frandon, M. A. Renucci, O. Briot, B. Gil, and R. L. Aulombard, Solid State Commun. **100**, 207 (1996).
[14]F. Demangeot, J. Frandon, P. Baules, F. Natali, F. Semond, and J. Massies, Phys. Rev. B **69**, 155215 (2004).
[15]V. Y. Davydov, N. S. Averkiev, I. N. Goncharuk, D. K. Nelson, I. P. Nikitina, A. S. Polkovnikov, A. N. Smirnov, M. A. Jacobson, and O. K. Semchinova, J. Appl. Phys. **82**, 5097 (1997).
[16]L. S. Wang, K. Y. Zang, S. Tripathy, and S. J. Chua, Appl. Phys. Lett. **85**, 5881 (2004).
[17]H. Y. Huang, Z. Y. Li, J. Y. Lu, Z. J. Wang, C. S. Wang, K. M. Lau, K. J. Chen, and T. Y. Zhang, J. Micromech. Microeng. **19**, 095019 (2009).
[18]J. J. Wortman and R. A. Evans, J. Appl. Phys. **36**, 153 (1965).
[19]K. Shimada, T. Sota, and K. Suzuki, J. Appl. Phys. **84**, 4951 (1998).
[20]R. Loudon, Adv. Phys. **13**, 423 (1964).
[21]D. Wang, Y. Dikme, S. Jia, K. J. Chen, K. M. Lau, P. van Gemmern, Y. C. Lin, H. Kalisch, R. H. Jansen, and M. Heuken, J. Cryst. Growth **272**, 489 (2004).
[22]D. Wang, S. Jia, K. J. Chen, K. M. Lau, Y. Dikme, P. van Gemmern, Y. C. Lin, H. Kalisch, R. H. Jansen, and M. Heuken, J. Appl. Phys. **97**, 056103 (2005).
[23]P. Perlin, C. Jauberthie-Carillon, J. P. Itie, A. S. Miguel, I. Grzegory, and A. Polian, Phys. Rev. B **45**, 83 (1992).
[24]A. R. Goñi, H. Siegle, K. Syassen, C. Thomsen, and J.-M. Wagner, Phys. Rev. B **64**, 035205 (2001).
[25]V. Y. Davydov, Y. E. Kitaev, I. N. Goncharuk, A. N. Smirnov, J. Graul, O. Semchinova, D. Uffmann, M. B. Smirnov, A. P. Mirgorodsky, and R. A. Evarestov, Phys. Rev. B **58**, 12899 (1998).